Development of Fe-based Catalysts for Purification of Coke Oven Gases

Z.R. Ismagilov[1], O.Yu. Podyacheva[1]*, L.T. Tzykoza[1], M. Sakashita[2], N.V. Shikina[1],

V.A. Ushakov[1], V.V. Kuznetsov[1], Sh. Tamura[2] and K. Fujimoto[3]

[1]Boreskov Institute of Catalysis, prosp. ak. Lavrentieva, 5, 630090 Novosibirsk, Russia

[2]Japan Technical Information Service, Sogo-kojimachi No 3 Bldg., 1-6 Kojimachi, Chiyoda-ku, 1020083 Tokyo, Japan

[3]Nippon Steel Co., 20-1 Shintomi, Futtsu-city, Chiba, 2938511, Japan

Abstract

Fe-based catalysts of different geometry are developed for the purification of coke oven gases: bulk, supported on alumina and supported on alumina silicate monoliths. Adsorption and decomposition of H_2S on the catalysts developed are studied. Influence of active component content, type of support material and modification by Mn and Mo on the catalyst activity in de-H_2S process is elucidated. Supported monolith catalysts show superior activity over bulk and supported spherical catalysts in H_2S decomposition reaction and demonstrate stable operation in ammonia decomposition process during 2 hours at 900°C giving 100% ammonia conversion.

Introduction

Main impurities of coke oven gases (COG) are H_2S and NH_3. More than 99% of these impurities, which form harmful products upon oxidation or processing of COG, have to be removed taking into account environmental and technological aspects. On the other hand, COG containing up to 60% of hydrogen is considered as essential source for production of pure H_2. Therefore, an efficient and low cost process for cleaning of COG is highly desirable.

According to literature data, many metal sulfides M_xS_y, where M = Na, K, Li, Fe, Co, Ni, Cr, Mo, V and metal oxides M_xO_y, where M = Fe, Cr, Cu, Mn, V, Ti Mo, Al, Zn are active in H_2S decomposition reaction [1-17]. When metal oxides are used, the fist step in the process of H_2S decomposition is the transformation of metal oxide into metal sulfide. Metal sulfide formed acts as a catalyst for the process of H_2S decomposition. It was found that metal sulfide made in result of treatment of metal oxide by H_2S shows superior activity compared with the ready-made metal sulfide in reaction conditions [5].

Different sulfides form the following order according to their activity in H_2S decomposition reaction: CoS_2[18]<MoS_2[19]<Co-Mo-S[20]<Ru-Mo-S[21]. It is necessary to note that besides Mo- and V-based catalysts, which are commonly studied in de-H_2S reaction, Fe_2O_3 catalyst also deserves attention as it exhibits high level of activity not only in H_2S decomposition process, but in ammonia decomposition reaction as well [11,13,14], making this catalyst very promising for the use in the complex cleaning of COG. In [17] a mixture of more than 10 oxides (Fe_2O_3, MnO_2, SiO_2, ZnO, CaO *et al.*) was studied in the H_2S decomposition reaction. It was shown that initially hydrogen sulfide is absorbed by the catalyst and as a consequence both hydrogen sulfide and hydrogen are not detected in the reaction mixture. During adsorption the catalyst transforms into metal sulfides and then decomposition of H_2S begins. It was concluded that the activity of this complex catalyst is determined primarily by Fe_2O_3 taking into account its relative high quantity in the catalyst (42.6 wt.%) and its capability of easy formation of sulfides compared with other oxides.

The subject of this paper is the development of Fe-based catalysts of different geometry for purification of coke oven gases.

*corresponding author. E-mail: pod@catalysis.nsk.su

Printed in Kazakhstan

Experimental

Bulk Fe_2O_3 catalysts were synthesized via thermal decomposition of different Fe-containing salts at 600°C, tableted and sieved to 1-2 mm (samples from F-1 to F-7, Table 1). Supported spherical catalysts were prepared by wetness impregnation of different supports by $Fe(NH_4)_3(C_2O_4)_3 \cdot 3H_2O$ solution and calcination at 600°C (samples from F-8 to F-11, Table 2). Spherical γ-Al_2O_3 (1-2 mm) and α-Al_2O_3 (2-3 mm), ZrO_2 and SiO_2 sieved to 1-2 mm were used as a support material for the deposition of active component. Modification of supported Fe-containing catalysts by Mn and Mo was performed by wetness impregnation of ready-made 2.9%Fe/γ-Al_2O_3 (F-8) and 4.1%Fe/α-Al_2O_3 (F-9) catalysts by the use of Mn $(NO_3)_2$ and $(NH_4)_6Mo_7O_{24}$ solutions (samples Mn/F-8, Mn/F-9 and Mo/F-8, Mo/F-9, Table 2). Prepared spherical catalysts F-8 (2.9wt.%Fe/γ-Al_2O_3) and F-9 (4.1wt.% Fe/α-Al_2O_3) were crushed into powder, deposited from suspension containing catalyst powder and γ-Al_2O_3 as a binder onto alumina silicate monoliths B and calcined at 600°C (samples F-8/B and F-9/B). Content of Fe introduced into Fe-8/B catalyst amounts to 0.23 wt.%, whereas in F-9/B catalyst – 0.33 wt.%.

Phase composition of the catalysts was registered by XRD using HZG-4 (Cu K_α radiation) diffractometer with copper radiation in the 2θ range of 10-70 degrees. Specific surface area of the samples was measured by BET method. Quantitative analysis of elements in supported spherical and monolith catalysts was performed by the use of method of atom-absorption spectroscopy.

Prepared catalysts were tested in a 1% H_2S-99% Ar flow. Catalyst was placed into quartz reactor, free volume of reactor was filled by sieved quartz (1-2 mm). Catalyst was treated in N_2 first at 150°C during 30 min and then at 600°C during 30 min. Activity test included activation of the catalysts by reaction mixture at 600°C till establishment of a steady outlet concentration of H_2S and subsequent study of H_2S decomposition at the temperatures of 600→700→800→900→800→700→600°C at residence time equal to 1 s. Duration of catalyst activation was characterized by value ρ representing total amount of H_2S (mmole) fed into the reactor divided by the weight of a catalyst sample at which a steady level of H_2S conversion is achieved.

Activity test in de-NH_3 reaction was performed as follows: catalyst was placed into quartz reactor, at first was treated in He at 150°C during 30 min, then at 600°C during 1 hour and catalyst activity was measured within temperature interval of 600-900°C. Both fresh catalyst and catalyst after activity test in H_2S decomposition reaction were tested in NH_3 decomposition reaction.

Table 1
Physical chemical properties of bulk Fe_2O_3 catalysts synthesized via thermal decomposition of different Fe-containing salts at 600°C

Sample	Initial salt of Fe	Fresh catalyst		Catalyst after activity test		
		XRD	S_{BET}, m^2/g	Total duration of activity test, hrs	XRD	S_{BET}, m^2/g
F-1	Iron(III) nitrate nanohydrate $Fe(NO_3)_3 \cdot 9H_2O$	α-Fe_2O_3	8.3	12	$Fe_{1-x}S$	0.14
F-2 (sublimated during calcination)	Iron(III) chloride $FeCl_3$					
F-3 (calcined at 700°C)	Ammonium iron(II) sulfate hexahydrate $Fe(NH_4)_2(SO_4)_2 \cdot 6H_2O$	α-Fe_2O_3	13.0	19		
F-4	Iron(III) oxalate pentahydrate $Fe_2(C_2O_4)_3 \cdot 5H_2O$	α-Fe_2O_3	8.3	10	Fe_7S_8	0.12
F-5	Ammonium iron(III) oxalate trihydrate $Fe(NH_4)_3(C_2O_4)_3 \cdot 3H_2O$	α-Fe_2O_3	2.9	33	Fe_7S_8	2.1
F-6	Iron(III) citrate hydrate $FeC_6H_5O_7 \cdot nH_2O$	α-Fe_2O_3 + Fe_3O_4	9.3	28	$Fe_{1-x}S$	~ 0
F-7	Ammonium iron(III) dihydrocitrate citrate hydrate $2FeC_6H_5O_7 \cdot NH_4C_6H_7O_7 \cdot nH_2O$	α-Fe_2O_3	6.7	50	$Fe_{1-x}S$	~ 0

Table 2
Physical chemical properties of supported spherical catalysts

Sample	Catalyst composition	$T_{calc.}$, °C	Fresh catalyst		Catalyst after activity test		
			XRD	S_{BET}, m^2/g	Total duration of activity test, hrs	XRD	S_{BET}, m^2/g
F-8	2.9%Fe/ γ-Al_2O_3	600	γ-Al_2O_3	200	16	Fe_7S_8 + γ-Al_2O_3	101
		900	γ-, δ-, α-Al_2O_3	112	40	γ-, δ-, θ-, α-Al_2O_3	86
F-8a	4.6%Fe/ γ-Al_2O_3	600	γ-Al_2O_3	165	14	Complex mixture of phases	110
F-8b	9.7%Fe/ γ-Al_2O_3	600	Solid solution Fe^{3+} in γ-Al_2O_3	116	24	$Fe_{1-x}S$ + δ-, α-Al_2O_3	84
		900	δ-, α-Al_2O_3	73		$Fe_{1-x}S$ + δ-, α-Al_2O_3	47
F-9	4.1%Fe/ α-Al_2O_3	600	α-Fe_2O_3 + α-Al_2O_3	8.6	19	Fe_7S_8 + α-Al_2O_3	7.8
		900	α-Fe_2O_3 + α-Al_2O_3	11	6	Fe_7S_8 + α-Al_2O_3	10
F-9a	3.1%Fe/ α-Al_2O_3	600	α-Fe_2O_3 + α-Al_2O_3	11	16	Fe_7S_8 + α-Al_2O_3	9
F-9b	3.7%Fe/ α-Al_2O_3	600	α-Fe_2O_3 + α-Al_2O_3	12	16	Fe_7S_8 + α-Al_2O_3	8.6
F-10	5%Fe/ZrO_2	600	α-Fe_2O_3 + ZrO_2	9.7	30	Solid solution Fe^{3+} in ZrO_2	3.3
F-11	6%Fe/SiO_2	600	Amorphous	540	6	$Fe_{1-x}S$ + amorphous SiO_2	320
Mn/F8	2.7%Mn/[2.9%Fe/ γ-Al_2O_3]	600	β-Mn_2O_3 (traces) + amorphous phase	185	25	MnS + γ-, δ-, α-Al_2O_3	79
Mn/F9	3.0%Mn/[4.1%Fe/ α-Al_2O_3]	600	α-Fe_2O_3 + α-Al_2O_3 + β-Mn_2O_3	14	25	MnS + α-Al_2O_3	11
Mo/F8	4.4%Mo/[2.9%Fe/ γ-Al_2O_3]	600	γ-Al_2O_3	192	16	MoS_2+$Fe_{1-x}S$ + γ-Al_2O_3	117
Mo/F9	3.6%Mo/[4.1%Fe/ α-Al_2O_3]	600	Fe_2MoO_z or $Fe_2(MoO_4)_3$ + α-Al_2O_3	8.1	17	MoS_2+$Fe_{1-x}S$ + α-Al_2O_3	8.3

Results and discussion

Bulk catalysts

XRD showed formation of α-Fe_2O_3 after calcination at 600°C in all samples, except sample F-6, synthesized via thermal decomposition of iron (III) citrate hydrate, where formation of additional phase Fe_3O_4 was registered, Table 1. Specific surface area of the samples varies within interval of 2.9-13.0 m^2/g.

Use of oxide catalyst for H_2S decomposition reaction requires preliminary activation of catalyst by means of H_2S adsorption in order to transform metal oxide into metal sulfide. Detailed study of H_2S adsorption on the catalysts developed was performed in order to clarify the process of sulfidation of metal oxide. These experiments were fulfilled at the temperature of 600°C in order to decrease the contribution of the H_2S decomposition reaction in the experiments. Main results on the H_2S adsorption on bulk Fe_2O_3 catalysts are given in Fig. 1 showing dependence of H_2S conversion (X_{H_2S}, %, left axis) and quantity of hydrogen produced due to H_2S decomposition reaction (C_{H_2}, vol.%, right axis) on the magnitude ρ. Value ρ at which a steady level of H_2S conversion is achieved, can characterize the duration of catalyst activation. At the beginning of the experiments H_2S conversion attained value near 100%. Meantime, hydrogen was not registered in the reaction mixture. Thus, it can be concluded that almost all hydrogen sulfide is quantitatively adsorbed and interacted with the catalyst. After certain period of time, different for each catalyst, the increase of H_2S concentration in reaction mixture with simultaneous

increase of hydrogen concentration is observed. It is obvious that chemical transformation of a catalyst proceeds during H_2S adsorption by formation of a new phase which is active in H_2S decomposition reaction. Indeed, XRD registered sulfidation of the catalysts with formation of iron sulfide after reaction (Table 1, Fig. 2). It is interesting to note that duration of catalyst activation for the samples studied is different. The longest activation period was registered for the sample F-7 prepared via thermal decomposition of ammonium iron(III) dihydrocitrate citrate, while the shortest – for the sample F-4 prepared via thermal decomposition of iron(III) oxalate pentahydrate.

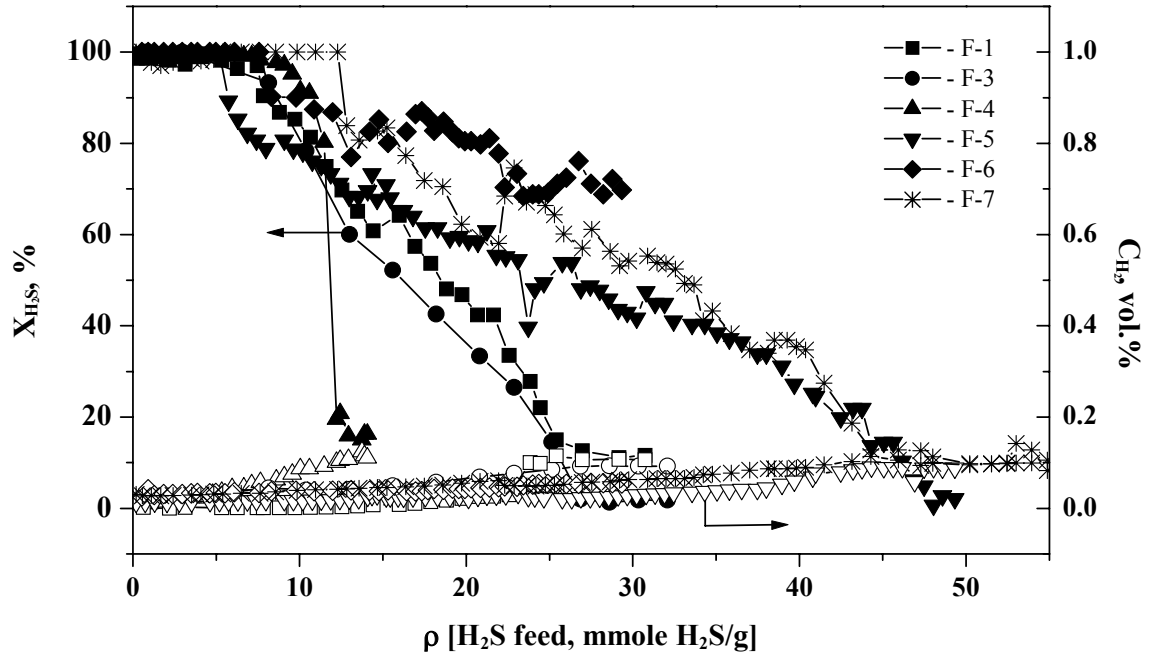

Fig. 1. Dependencies of H_2S conversion and quantity of H_2 produced (vol.%) on different bulk Fe_2O_3 catalysts (see Table 1). ρ represents amount of H_2S supplied (mmole) related to the 1 g of the sample.

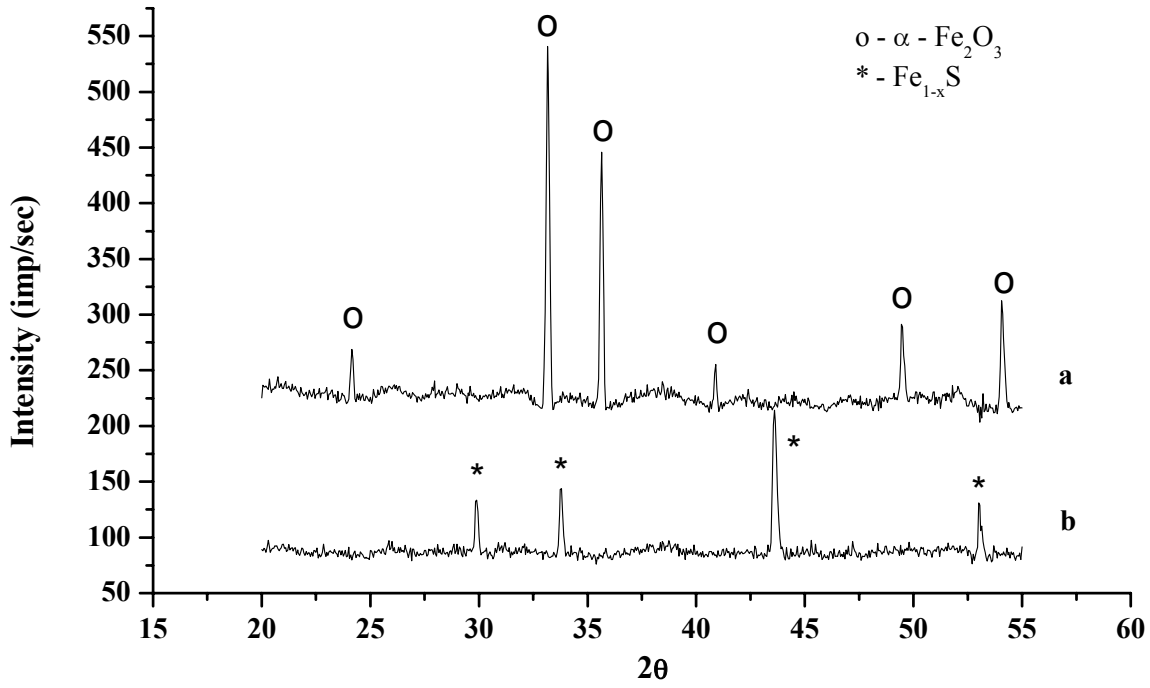

Fig. 2. XRD patterns of bulk F-1 catalyst: a – fresh catalyst, b – catalyst after activity test.

Calculated reaction rates of H_2 formation according to the decomposition reaction $H_2S \rightarrow H_2 + S$ on bulk Fe_2O_3 catalysts are given in Fig. 3. Histogram of reaction rate of H_2 formation related to the 1 g of the sample (mole H_2/s·g) demonstrates that Fe_2O_3 catalyst synthesized via thermal decomposition of iron(III) nitrate nanohydrate (F-1) is the most effective. Essential decrease of specific surface area of the samples after activity test (down to ~ 0 for F-6 and F-7) is observed (Table 1). The sample F-5 synthesized via thermal decomposition of ammonium iron (III) oxalate trihydrate demonstrates the highest thermal stability in respect to specific surface area. Although the catalysts F-1, synthesized via thermal decomposition of iron (III) nitrate nanohydrate, exhibited the highest activity in H_2S decomposition reaction, the ammonium iron (III) oxalate trihydrate was chosen for the preparation of supported catalysts in order to exclude emission of toxic nitrogen oxides which are formed during iron (III) nitrate nanohydrate decomposition. Moreover, the sample F-5 synthesized by the use of $Fe(NH_4)_3(C_2O_4)_3 \cdot 3H_2O$ shows sufficiently high activity in H_2S decomposition reaction and demonstrates the highest thermal stability in respect to specific surface area.

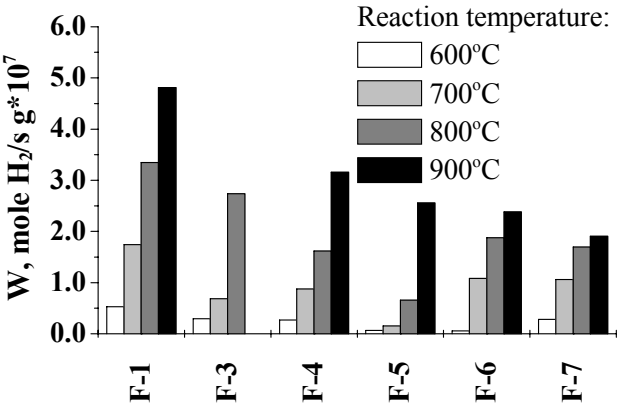

Fig. 3. Histogram of reaction rates of H_2 formation on bulk Fe_2O_3 catalysts synthesized via thermal decomposition of different Fe-containing salts at 600°C.

Supported spherical catalysts

Phase composition of spherical catalysts depends on the content of iron introduced and type of support material used (Table 2). Phase of α-Fe_2O_3 was registered in the catalysts supported on α-alumina and zirconia, while active component in the catalyst F-8b (9.7%Fe/γ-Al_2O_3) was recognized as the solid solution of Fe^{3+} in γ-Al_2O_3.

Activity of the catalysts supported on γ-Al_2O_3 and α-Al_2O_3 depends significantly on the content of active component, Fig. 4. Reaction rate of H_2 formation decreases with increase of Fe content in the sample for catalysts supported on γ-Al_2O_3. Highest activity demonstrates catalyst F-8 with Fe content equal to 2.9%. On the contrary, increase of Fe content from 3.1 to 4.1% in the catalyst F-9 leads to increase of the catalyst activity.

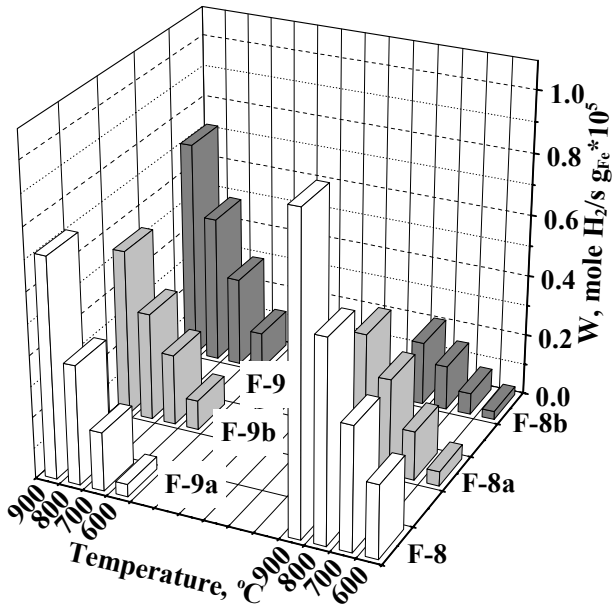

Fig. 4. Histogram of reaction rates of H_2 formation related to 1 g of Fe in the sample for supported spherical catalysts calcined at 600°C: F-8, F-8a, F-8b; and F-9a, F-9b, F-9 (see Table 2).

Formation of iron sulfide (Fe_7S_8 or $Fe_{1-x}S$) was registered in the samples after H_2S decomposition reaction for all catalysts supported both on γ- and α-Al_2O_3. The catalyst F-8a (4.6%Fe/γ-Al_2O_3) is the only exception. Transformation of oxide active component to iron sulfide leads to change of catalyst colour from beige (F-8) or orange (F-9) to black colour. Significant decrease of specific surface area of the samples supported on γ-Al_2O_3 is observed.

Activity data for Fe-containing catalysts supported on various materials (γ-Al_2O_3, α-Al_2O_3, ZrO_2, SiO_2) and calcined at 600°C are presented in Fig. 5. Increase of H_2S conversion with temperature rising from 600 to 900°C is observed. Meantime, the catalysts deposited both on γ-Al_2O_3 and α-Al_2O_3 demonstrate the highest level of activity. Formation of iron sulfide after activity test is registered for catalysts supported on γ-Al_2O_3, α-Al_2O_3 and SiO_2 materials,

whereas decrease of specific surface area is observed for all catalysts (Table 2).

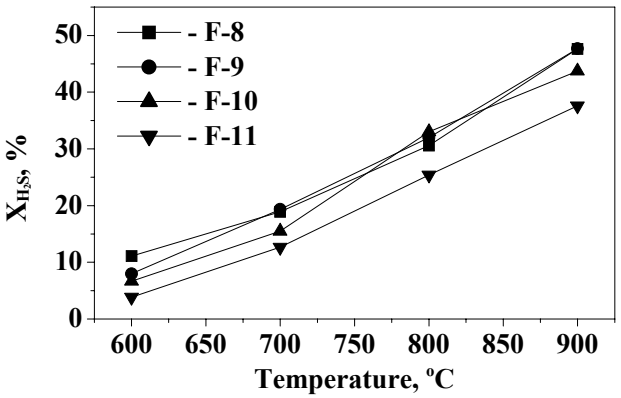

Fig. 5. Temperature dependencies of H_2S conversion on Fe containing catalysts supported on different materials and calcined at 600°C: F-8, F-9, F-10, F-11 (see Table 2).

Modification of the samples F-8 (2.9%Fe/γ-Al_2O_3) and F-9 (4.1%Fe/α-Al_2O_3) was performed to increase their activity. According to XRD analysis, modification of catalysts by manganese leads to formation of additional β-Mn_2O_3 phase compared with phase composition of initial catalysts (Table 2). Modification of F-8 by molybdenum does not change phase composition of the catalysts. XRD registers γ-Al_2O_3 similarly to initial F-8 catalyst. In turn, modification of F-9 sample by molybdenum changes significantly phase composition of the catalyst: interaction of Fe with Mo occurs leading to the formation of Fe_2MoO_z or $Fe_2(MoO_4)_3$ phases. However, activity data, presented in Fig. 6, allows to conclude that modification of the samples F-8 and F-9 by Mn and Mo results in decrease of the catalyst activity, although formation of MnS and MoS_2 is observed after activity test according to XRD data (Table 2).

Supported monolith catalysts

To clarify the influence of catalyst geometry on its activity in H_2S decomposition process, comparative analysis of activity data for different catalysts was made: bulk Fe_2O_3 catalyst F-5, supported spherical F-8, F-9 and supported monolith catalysts F-8/B, F-9/B (Fig. 7). Activity of supported spherical catalysts (F-8 and F-9) exceeds activity both of bulk and supported monolith catalysts. But it is necessary to emphasize that content of introduced active component (Fe) in the catalysts compared varies within wide range: 70 wt.% for bulk Fe_2O_3 catalyst and less than 1 wt.% for supported monolith catalysts. In order to consider this fact, reaction rates of H_2 formation reaction related to the 1 g of introduced Fe were compared. It is seen that picture is changed significantly. Supported monolith catalysts show superior activity compared with bulk and supported spherical catalysts, Fig. 7.

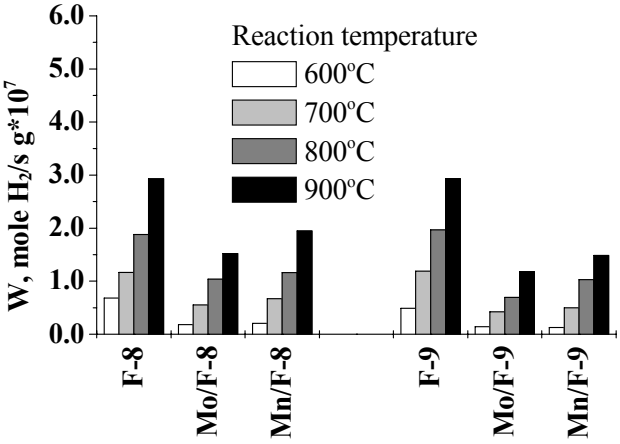

Fig. 6. Histogram of reaction rates of H_2 formation related to 1 g of sample for supported spherical catalysts F-8 and F-9 modified by Mo and Mn, calcined at 600°C: Mo/F-8, Mn/F-8, Mo/F-9, Mn/F-9 (see Table 2).

Results described above were devoted to the study of catalysts in H_2S decomposition reaction. However, besides H_2S, COG contain substantial amount of ammonia. Therefore, independent experiments on decomposition of ammonia by the use of monolith F-9/B catalyst were performed. In order to elucidate the behavior of catalysts in the presence of H_2S and NH_3,

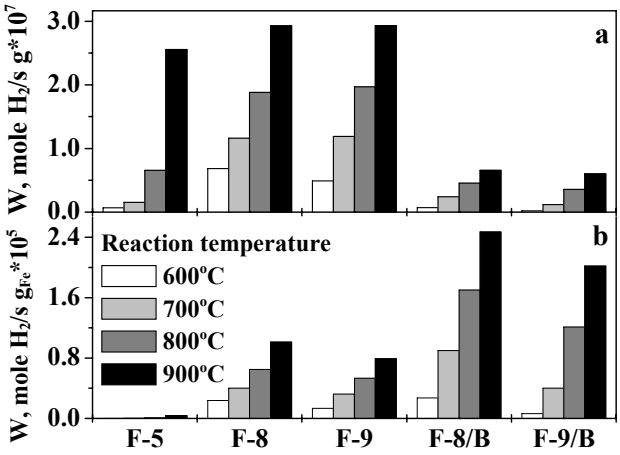

Fig. 7. Histogram of reaction rates of H_2 formation related to 1 g of the sample (a) and reaction rates of H_2 formation related to 1 g of Fe in the sample (b) for Fe-containing catalysts of different geometry calcined at 600°C: bulk F-5; supported spherical F-8 and F-9; supported monolith F-8/B and F-9/B.

activity of fresh catalysts was compared with activity of catalyst tested preliminary in H_2S decomposition reaction at the temperatures of 600→900→600°C. It was found that 100% ammonia conversion on the fresh supported monolith catalyst is observed starting from 750-800°C, whereas for catalyst after de-H_2S test – starting from 900°C, Fig. 8. Monolith catalyst demonstrated stable operation in de-NH_3 process at 900°C for 2 hours.

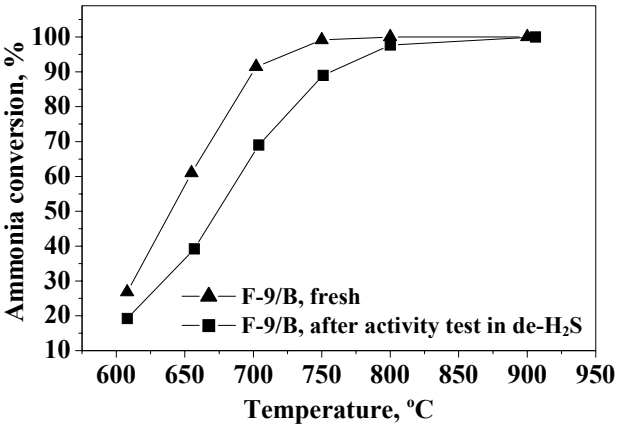

Fig. 8. Temperature dependencies of ammonia conversion on supported monolith catalyst F-9/B at GHSV=3600 h^{-1}.

Conclusions

Fe-based catalysts of different geometry are developed for the purification of coke oven gases: bulk, supported on alumina and supported on alumina silicate monoliths.

Adsorption and decomposition of H_2S reaction were studied on bulk Fe_2O_3 catalyst and $Fe(NH_4)_3(C_2O_4)_3 \cdot 3H_2O$ salt was chosen as the best starting material to be used for the synthesis of supported catalysts. Fe-containing catalysts supported on alumina show highest level of activity in H_2S decomposition process compared with Fe-containing catalysts supported on ZrO_2 and SiO_2. It was found that modification of Fe-containing catalysts by Mn and Mo leads to the decrease of the catalyst activity.

Monolith catalysts synthesized show superior activity in de-H_2S process over bulk and spherical catalysts when reaction rates of H_2 formation related to 1 g of Fe introduced are compared. It was revealed that monolith catalysts demonstrate stable operation in ammonia decomposition process during 2 hours at 900°C giving 100% ammonia conversion.

Acknowledgements

This work was supported by NEDO project in 2000-2001, Japan. The authors would like to thank PhD student A.W. Aberle for carrying out the de-NH_3 test of two samples.

References

1. Chivers, T., Hyne, J., Lau, C. *et al.*, Int. J. Hydrogen Energy 5:499 (1980).
2. Chivers, T., Lau, C. *et al.*, Int. J. Hydrogen Energy 10:21 (1985).
3. Chivers, T., Lau C. *et al.*, Int. J. Hydrogen Energy 12:561 (1987).
4. Al-Shamma, L.M., Naman, S.A., Int. J. Hydrogen Energy 14:173 (1989).
5. Al-Shamma, L.M., Naman, S.A., Int. J. Hydrogen Energy 15:1 (1990).
6. Lee, Y.S., Kim, H.T., Yoo, K.O., Ind. Eng. Chem. Res. 34:1181 (1995).
7. Fukuda, K, Dokiya, M. *et al.*, Ind. Eng. Chem. Fundam. 17:243 (1978).
8. Zaghigalov, V.A., Gerei, S.V., Rubanik, M.Ya., Kinetics and Catalysis 16:967 (1975).
9. Zaman, J., Chakma, A., Fuel Process Technol. 41:159 (1995).
10. Yang, B.L., Kung, H.H., Ind. Eng. Chem. Res. 33:1090 (1994).
11. US Patents: 4273749 (1981).
12. US Patents: 5188811 (1993).
13. US Patents: 5632964 (1997).
14. US Patents: 5679313 (1997).
15. Wakker, J.P., Gerritsen, A.W., Moulijn, J.A., Ind. Eng. Chem. Res. 32:139 (1993).
16. Bishara, A., Salman O.A., Int. J. Hydrogen Energy12:679 (1987).
17. Yumura, M., Furimsky, E., Appl. Catal. 16:157 (1985).
18. Meeyoo, V., Adesina, A.A., Foulds, G., Chem. Eng. Commun. 144:1 (1996).
19. Koloidas, V.E., Papayannakos, N.G., Ind. Eng. Chem. Res. 30:345 (1991).
20. Moffat, S.C., Adesina, A.A., Catal. Lett. 37:167 (1996).
21. Gwaunza, M., Adesina, A.A., React. Kinet. Catal. Lett. 62:55 (1997).

Received 8 June 2003.